Mon. Not. R. Astron. Soc. **384,** 1158–1164 (2008) doi:10.1111/j.1365-2966.2007.12788.x

Formation of CO_2 on a carbonaceous surface: a quantum chemical study

T. P. M. Goumans, Madeeha A. Uppal and Wendy A. Brown★

Department of Chemistry, University College London, 20 Gordon Street, London WC1H 0AJ

Accepted 2007 November 27. Received 2007 November 22; in original form 2007 August 29

ABSTRACT

The formation of CO_2 in the gas phase and on a polyaromatic hydrocarbon surface (coronene) via three possible pathways is investigated with density functional theory. Calculations show that the coronene surface catalyses the formation of CO_2 on model grain surfaces. The addition of ^3O to CO is activated by 2530 K in the gas phase. This barrier is lowered by 253 K for the Eley–Rideal mechanism and 952 K for the hot-atom mechanism on the surface of coronene. Alternative pathways for the formation of CO_2 are the addition of ^3O to the HCO radical, followed by dissociation of the HCO_2 intermediate. The O + HCO addition is barrierless in the gas phase and on the surface and is more than sufficiently exothermic to subsequently cleave the H–C bond. The third mechanism, OH + CO addition followed by H removal from the energized HOCO intermediate, has a gas-phase exit barrier that is 1160 K lower than the entrance barrier. On the coronene surface, however, both barriers are almost equal. Because the HOCO intermediate can also be stabilized by energy dissipation to the surface, it is anticipated that for the surface reaction the adsorbed HOCO could be a long-lived intermediate. In this case, the stabilized HOCO intermediate could react, in a barrierless manner, with a hydrogen atom to form $H_2 + CO_2$, HCO_2H, or $H_2O + CO$.

Key words: astrochemistry – molecular processes – ISM: molecules.

1 INTRODUCTION

Carbon dioxide (CO_2) ices have long been observed in the interstellar medium (d'Hendecourt & Jourdain de Muizon 1989). The much higher abundance of solid CO_2 than gas phase CO_2, when compared to the solid to gas-phase ratios of CO and H_2O, (van Dishoeck et al. 1996; Boonman et al. 2003) indicates that CO_2 is formed predominantly on grain surfaces rather than forming in the gas phase and then freezing out. Experiments have shown that particle or ultraviolet irradiation of CO and CO/H_2O are efficient pathways to form CO_2 (d'Hendecourt et al. 1986; Grim et al. 1989; Moore, Khanna & Donn 1991; Gerakines, Schutte & Ehrenfreund 1996; Allamandola, Bernstein & Sanford 1997). However, solid CO_2 has also been observed towards quiescent dark clouds (Whittet et al. 1998), which calls for efficient CO_2 formation on surfaces without energizing or ionizing events. Experimental studies of the direct addition mechanism (equation 1), followed by stabilization through collisions or luminescence, have hitherto been inconclusive:

$$^3O + CO \rightarrow \left[^3CO_2\right]* \rightarrow CO_2 + h\nu \\ + M \rightarrow CO_2. \quad (1)$$

Fournier et al. (1979) found that upon irradiation of N_2O/CO in an argon matrix, $^3CO_2$ was efficiently formed from ^3O and CO. However, in later studies (Grim & d'Hendecourt 1986; Roser et al. 2001) no efficient formation of CO_2 was observed upon irradiating CO ice with cold oxygen atoms, implying that the addition reaction is activated, with an estimated barrier of 290 K (Roser et al. 2001). The activation barrier for the direct addition on a surface can easily be overcome if kinetically hot oxygen atoms are used, as recently shown by Madzunkov et al. (2006). The measured activation barrier in the gas phase is much higher (1400–3600 K), although these values are often extracted from complicated reaction schemes (Tsang & Hampson 1986; Fujii et al. 1987). Recent high-level calculations predict a barrier of 2970 K (Talbi, Chandler & Rohl 2006) for mechanism (1) in the gas phase.

Because the $^3O + CO$ addition has a considerable activation barrier, two alternative pathways for CO_2 formation have been put forward (Ruffle & Herbst 2001):

$$^3O + HCO \rightarrow H + CO_2, \quad (2)$$

$$OH + CO \rightarrow H + CO_2. \quad (3)$$

Both reactions have been studied previously in view of their importance in combustion chemistry. Reaction (2) is unactivated and yields $H + CO_2$ or $OH + CO$ at a rate of 5×10^{-11} cm^3 molecule^{-1} s^{-1} (Baulch et al. 2005) with approximately equal branching between $H + CO_2$ and $OH + CO$ (Campbell & Handy 1978). The characteristics of reaction (3), which proceeds via an energetic HOCO intermediate, have been studied extensively using both theory (Yu, Muckerman & Sears 2001; Chen & Marcus 2005; Fabian & Janoschek 2005; Song et al. 2006; Valero & Kroes 2006, and

★E-mail: w.a.brown@ucl.ac.uk

references therein) and experiment (Frost, Sharkey & Smith 1993; Fulle et al. 1996; Golden et al. 1998; Baulch et al. 2005, and references therein).

In the chemical network model of Ruffle & Herbst (2001), reaction (1) has a negligible rate at 10–20 K because of its estimated barrier of 1000 K, reaction (2) is barrierless and a barrier of 80 K is assumed for reaction (3). In order to reproduce the CO_2 abundances observed towards Elias 16, the barrier of reaction (1) had to be lowered to 130 K (Ruffle & Herbst 2001).

Currently, there is no knowledge of how surfaces influence reactions (1)–(3), but a recent computational study has shown that two isolated water molecules do not affect the activation barrier for the $^3O + CO$ addition (Talbi et al. 2006). A detailed understanding of the mechanisms of reactions (1)–(3) on a surface could improve chemical gas–grain networks such as the OSU data base (http://www.physics.ohio-state.edu/∼eric). In this paper we assess the influence of a carbonaceous surface on the CO_2 formation pathways (1)–(3) using computational chemistry. As a model for a grain surface we use coronene, a polycyclic aromatic hydrocarbon (PAH) consisting of a central six-membered ring, surrounded by six other six-membered rings. PAHs have been indicated as models for amorphous carbon observed in carbonaceous grains (Scott & Duley 1996).

2 COMPUTATIONAL METHODOLOGY AND VALIDATION

Density functional theory (DFT) calculations have been performed using GAUSSIAN 03 (Frisch et al. 2004). We validated our methodology by considering the adsorption energy of CO on coronene and the activation barrier for the gas-phase reaction of $^3O + CO$. The MPWB1K functional, which has been benchmarked for weak interactions as well as activation energies (Zhao & Truhlar 2004), with a 6-311G∗ basis set and an ultrafine integration grid appeared most suitable for our calculations. A polarization function was added to the hydrogen atom of the reacting system (reactions 2 and 3). We have also included scaled zero-point energies (0.9537, scaling factor for a 6-31+G* basis; Zhao & Truhlar 2004). Various adsorption modes have been considered for all reactants and products, focusing on adsorption on the central ring of coronene.

We first considered the B97-1 functional (Hamprecht et al. 1998), which has been indicated to perform well for barriers in astrochemical reactions (Andersson & Grüning 2004) as well as for weak interactions (Zhao & Truhlar 2005). However, this functional gives a negative activation barrier for the $^3O + CO$ reaction in the gas phase with a long-range complex intermediate. A more detailed investigation of several functionals indicated that a hybrid functional with a high percentage of Hartree–Fock exchange (usually denoted 'K' for kinetic) is necessary to reproduce the high-level *ab initio* activation energy [CCSD(T)/cc-pV5Z] of Talbi et al. (2006). Subsequently we focused on the MPWB1K and the MPW1K functionals, which both give activation energies in agreement with the values of Talbi et al. (2006). Furthermore, both of these functionals contain the modified Perdew–Wang exchange functional which has been designed to reproduce some van der Waals interaction (Adamo & Barone 1998). Although with these functionals the interaction of CO with coronene is not very strong and lower than the experimental value for adsorption on graphite (see below), MPWB1K yielded the largest adsorption energies. A Pople basis set with diffuse functions (6-31+G*) yielded imaginary frequencies for coronene, therefore we used the triple zeta 6-311G*(*) basis instead. Activation and reaction energies are given to three significant digits in temperature units (K), where 1 K = 0.008 3145 kJ mol^{-1}. For the Langmuir–Hinshelwood mechanisms we adsorbed both reactants on the centre of the ring and found the transition states that yield the required product. Because of the relatively low adsorption energies we assume that for reactions that have gas-phase barriers, the activation barriers are rate determining, rather than the diffusion of the reactants on the surface being the rate-determining step. Our coronene model is too small to calculate accurate diffusion barriers on a graphitic surface, but from the different adsorption geometries considered, the barrier for diffusion appears to be quite small for O, OH and CO. The activation and reaction energies for a Langmuir–Hinshelwood reaction are thus reported with respect to CO or CO_2 adsorbed on coronene, with the adsorption energy of the coreactant subtracted.

Table 1. Activation ($\Delta E^{\ddagger}$) and reaction energies ($\Delta E^{\rm rxn}$) for gas-phase reactions (1)–(3). MPWB1K/6-311G* + ZPE energies in K.

Reaction	Step	$\Delta E^{\ddagger}$	$\Delta E^{\rm rxn}$
(1)	$^3O + CO \rightarrow {}^3CO_2$	2530	−11 100
(2)	$^3O + HCO \rightarrow {}^2HCO_2$	0	−47 900
	$^2HCO_2 \rightarrow H + CO_2$	1160	−6300
(3)	$OH + CO \rightarrow t$-HOCO	−82	−14 200
	t-HOCO $\rightarrow c$-HOCO	4340	533
	c-HOCO $\rightarrow H + CO_2$	12 800	−588
	$OH + CO \rightarrow H + CO_2$	−902[a]	−14 300

[a]Exit channel barrier with respect to reactants.

3 GAS-PHASE REACTIONS

We have summarized the gas-phase energy profiles for the three mechanisms proposed to contribute to CO_2 formation in Table 1.

The calculated activation energy for reaction (1) is 2530 K, slightly lower than the high-level *ab initio* value of 2970 K (Talbi et al. 2006). For reaction (2), the addition of ^3O to HCO is barrierless and the barrier along the H–CO_2 dissociation coordinate is 1160 K above the ground-state energy of the HCO_2 intermediate. This barrier could be easily overcome, however, with the excess energy from the exothermic formation (47 900 K) of HCO_2 from O + HCO (Fig. 1). Therefore, reaction (2) is thought to be an efficient route to CO_2 formation in the gas phase.

The mechanism for reaction (3) is complex (Frost et al. 1993; Fulle et al. 1996), proceeding via a hydrogen-bonded collision

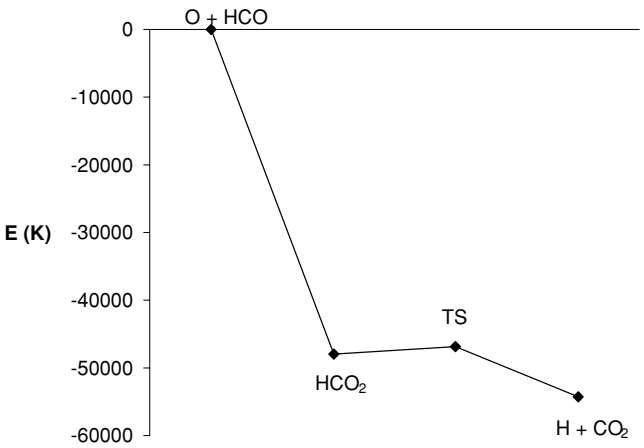

Figure 1. Gas-phase reaction pathway for mechanism (2) with relative energies in K. TS = transition state.

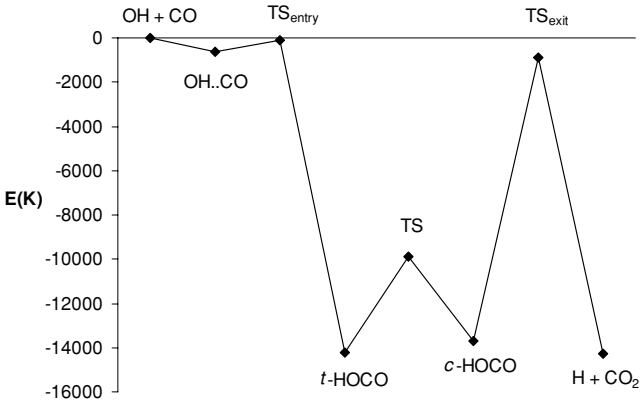

Figure 2. Gas-phase reaction pathway for mechanism (3) with relative energies in K. TS = transition state.

complex through a transition state to *t*-HOCO. This intermediate can be collisionally stabilized, react back to OH + CO, or continue to the products H + CO_2. In the last case the complex will first have to isomerize to *c*-HOCO before dissociation to H + CO_2 takes place (Fig. 2). The dynamics of this reaction are determined by the relative energy of the entrance transition state (OH + CO) and exit transition state (*c*-HOCO → H + CO_2) with respect to the separated reactants (Chen & Marcus 2005). In general, the MPWB1K/6-311G** potential energy surface for OH + CO is in good agreement with previous high-level *ab initio* results (Yu et al. 2001) up to the formation of *c*-HOCO. However, our calculations predict the exit channel to be slightly lower than the reactants (−820 K) whereas previous calculations predict it to be higher than the reactants, at about +720 K. Furthermore, the products H + CO_2 are overstabilized at our level of calculation. The difficulties of using DFT to study the OH + CO reaction have been noted previously by Andersson & Grüning (2004). Since the relative barrier height of this exit channel with respect to the reactants is important in the formation of CO_2 from cold OH + CO, our calculations will be only a qualitative measure to assess the influence of a carbonaceous surface on this potential energy surface.

4 INFLUENCE OF THE CORONENE SURFACE ON CO_2 FORMATION

We have summarized the reaction energies and relevant activation energies for reactions (1)–(3) on a coronene surface in Table 2. We consider the Eley–Rideal, Langmuir–Hinshelwood and hot-atom mechanisms for activated reaction (1). For reactions (2) and (3) we only report the energies for the Langmuir–Hinshelwood mechanism. The first step of reaction (2), ^3O + HCO, is barrierless for all mechanisms.

Table 2. Activation ($\Delta E^{\ddagger}$) and reaction energies (ΔE^{rxn}) for surface reactions (1)–(3). MPWB1K/6-311G* + ZPE energies in K. ER = Eley–Rideal, LH = Langmuir–Hinshelwood, HA = hot-atom mechanism.

Reaction	Step	$\Delta E^{\ddagger}$	ΔE^{rxn}
(1) ER	$^3O_g + CO_{ads} \rightarrow {}^3CO_{2,ads}$	2280	−11 800
(1) LH	$^3O_{ads} + CO_{ads} \rightarrow {}^3CO_{2,ads}$	2400	−11 000
(1) HA	$^3O^*_{ads} + CO_{ads} \rightarrow {}^3CO_{2,ads}$	1580	−11 800
(2) LH	$^3O_{ads} + HCO_{ads} \rightarrow {}^2HCO_{2,ads}$	0[a]	−48 500
	$^2HCO_{2,ads} \rightarrow H_{ads} + CO_{2,ads}$	1090	−5730
(3) LH	$OH_{ads} + CO_{ads} \rightarrow t\text{-}HOCO_{ads}$	−229	−14 900
	$OH_{ads} + CO_{ads} \rightarrow H_{ads} + CO_{2,ads}$	−408[b]	−13 500

[a]Barrierless for both Eley–Rideal and Langmuir–Hinshelwood mechanisms. [b]Exit channel barrier with respect to reactants.

4.1 ^3O + CO

CO can adsorb in various geometries on the central coronene ring, with adsorption energies in the region of 400 K. The preferred geometry is with the CO adsorbed in the centre of the aromatic ring with the CO bond parallel to the surface at about 3.0 Å (as in Fig. 3). The adsorption energy of 410 K is substantially lower than the experimentally determined value of 1300–1560 K for CO adsorption on graphite (Piper, Morrison & Peters 1984; Ulbricht et al. 2006). This discrepancy could be due to the measured value also including CO–CO interactions on the surface, the nature of the surface (coronene versus graphite), as well as an underestimation of the weak physisorption interactions by the MPWB1K functional. Since our computational model appears to underestimate physisorption energies, any effect we do find on catalysis could be enlarged if the true, stronger, interaction is considered. Where our model predicts a positive catalytic effect, for instance for $^3O_g + CO_{ads}$ (see below), we expect the actual barrier to be lowered more if the physisorption of CO is enhanced. For reactions that follow a Langmuir–Hinshelwood mechanism, a stronger physisorption interaction could induce a sizeable barrier for diffusion. In a recent study, the potential energy surface for diffusion of a hydrogen atom has been estimated at 46 K, one-fifth of the adsorption energy, from high-level calculations on the different adsorption sites on coronene (Bonfanti et al. 2007). Heavier atoms and molecules will have larger adsorption energies and diffusion barriers, which could restrain reactions from taking place via the Langmuir–Hinshelwood mechanism. However, when a reactant is created on the surface via an energetic process, such as OH formed from photodissociation of H_2O, the energized particle can travel quite large distances on top of the surface (Andersson et al. 2006).

When CO is physisorbed on coronene, gas-phase ^3O can react with it in an Eley–Rideal type mechanism (Fig. 3). The barrier for this reaction is 2280 K, i.e. 253 K lower than in the gas phase, demonstrating the catalytic effect a carbonaceous surface can exert even though the interaction of CO with this surface is weak.

Alternatively, oxygen atoms could also adsorb on the coronene surface and then react with CO in a Langmuir–Hinshelwood type reaction. Therefore, we also investigated the adsorption modes of oxygen atoms on the coronene surface. Triplet oxygen atoms physisorb preferentially in the bridged position with an adsorption energy of 820 K. Electronically excited singlet oxygen atoms chemisorb without a barrier, giving rise to a three-member C–C–O ring. Our calculations show that the triplet–singlet crossing along this chemisorption mode occurs at about 10 000 K above the ground-state energy of the reactants, thus ensuring that cold oxygen atoms in their ground triplet state will only physisorb on a carbonaceous surface. The transition state for CO_2 formation when both reactants are physisorbed on the surface (Fig. 4) is lower in energy than the Eley–Rideal transition state by 698 K. Consequently, if physisorbed oxygen atoms have not equilibrated with the surface ('hot-atom mechanism'), the ^3O + CO barrier is reduced to 1580 K. If the oxygen atoms are thermalized on the surface, the reaction proceeds via a pure Langmuir–Hinshelwood mechanism, heightening the barrier to 2400 K, only slightly lower than the gas-phase barrier. In summary, calculations show that a carbonaceous surface catalyses the ^3O + CO addition reaction, lowering the gas-phase barrier to 2280 K

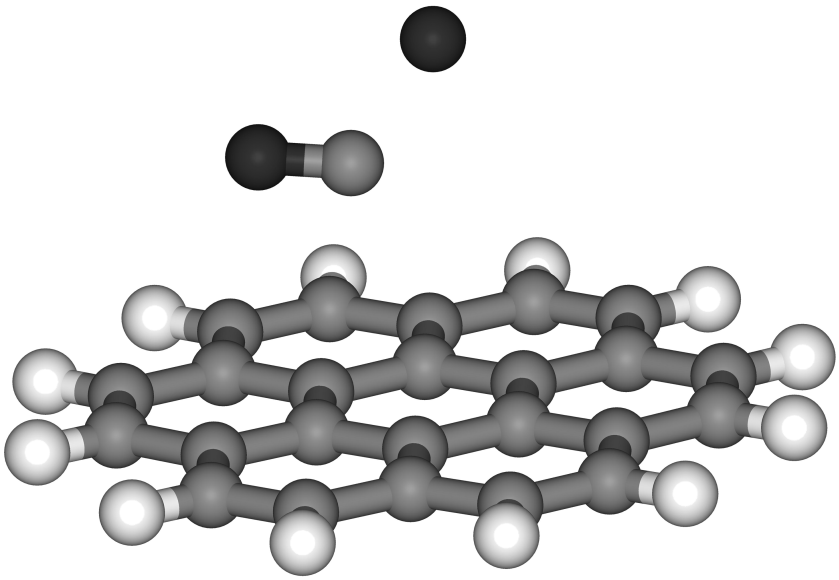

Figure 3. Eley–Rideal transition state for $^3O + CO$ on a coronene surface. Black atoms: O, grey: C, white: H.

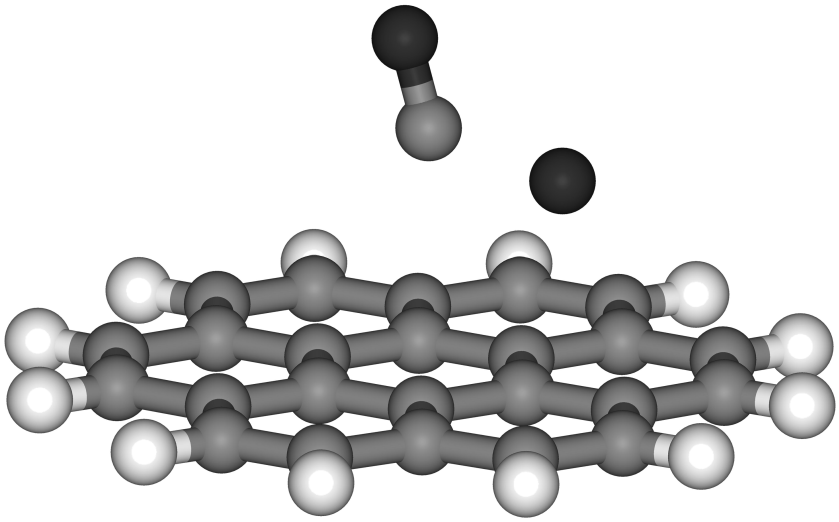

Figure 4. Langmuir–Hinshelwood transition state for $^3O + CO$ on a coronene surface. Black atoms: O, grey: C, white: H.

for the Eley–Rideal mechanism and to 1580 K for the hot-atom mechanism.

4.2 $^3O + HCO$

HCO has a physisorption energy of 966 K and preferentially adsorbs on coronene with a hydrogen atom pointing towards the surface. Quick potential energy surface scans indicate that the addition of ^3O to adsorbed HCO still proceeds in a barrierless manner on the coronene surface, with the reaction exothermicity lowered to −48 500 K. The resulting HCO_2 intermediate preferentially adsorbs with the hydrogen atom pointing towards the surface, with an adsorption energy of 1410 K. Removal of the hydrogen atom from this intermediate occurs with a barrier of 1090 K with respect to the ground-state energy, close to the gas-phase barrier. Only if the HCO_2 intermediate could transfer its substantial excess energy from the formation reaction rapidly and completely to the surface would this barrier be insurmountable at the temperatures in the interstellar medium. Since intramolecular energy transfer is at best as fast as internal conversion, which results in the breaking of the H–CO_2 bond, it is likely that reaction (2) will proceed to yield $H + CO_2$, both in the gas phase and on a surface.

4.3 OH + CO

OH physisorbs on coronene with an energy of 1220 K and, like HCO, preferentially adsorbs with the hydrogen atom slanted towards the surface. The Langmuir–Hinshelwood activation energy for the entrance barrier leading to adsorbed *t*-HOCO is slightly lowered from −82 K in the gas phase to −229 K with respect to OH_{ads} and CO_{ads}. On the surface the exit barrier lies closer to the entrance barrier (−408 K, with respect to OH_{ads} and CO_{ads}).

Unlike reaction (2), where the exothermicity of the first reaction step more than suffices to overcome the subsequent barrier, the exothermicity of the first step in reaction (3) is barely sufficient to overcome the final barrier (exit channel *c*-HOCO → $H + CO_2$).

Therefore if only a fraction of the excess energy is transferred to the surface, the adsorbed HOCO intermediate will be stabilized and not react further, just as observed under high-pressure experimental conditions (Golden et al. 1998). However, our calculations indicate that both in the gas phase and on the surface a stabilized (adsorbed) HOCO intermediate can subsequently react in a barrierless manner with an additional hydrogen atom to yield $H_2 + CO_2$, $H_2O + CO$ or HCO_2H (formic acid). Which of these three pairs of products is formed depends only on the orientation of the HOCO intermediate and the incoming hydrogen atom. The reaction of OH + CO on a surface could therefore potentially yield CO_2 via the stabilized HOCO intermediate reacting with another incoming hydrogen atom.

5 ASTROPHYSICAL CONSEQUENCES

We have investigated the influence of a carbonaceous surface on the three suggested routes for CO_2 formation (reactions 1–3). In the gas phase the activated (2530 K) addition of cold ground-state oxygen atoms to CO (reaction 1) is a negligible route to CO_2 formation in the coldest regions of the interstellar medium. On a carbonaceous surface, however, this barrier is lowered to 2280 K for the Eley–Rideal mechanism and to 1580 K for the hot-atom mechanism.

The reaction of CO_{ads} with ^3O competes with desorption of CO from the surface. The propensity of CO_{ads} to react with ^3O rather than desorb can be evaluated by assessing the ratio of the rates for these two processes:

$$\frac{r_{\rm rxn}}{r_{\rm des}} = \frac{k_{\rm rxn}\theta_{\rm CO}[{\rm O}]}{k_{\rm des}\theta_{\rm CO}} = \frac{A_{\rm rxn}}{A_{\rm des}}[{\rm O}]\exp\left(\frac{-\Delta E^{\ddagger}_{\rm rxn} + \Delta E^{\ddagger}_{\rm des}}{T}\right). \quad (4)$$

In equation (4) θ_{CO} is the surface concentration of CO in mol m^{-2}, [O] is the concentration of ^3O atoms in mol m^{-2} or mol m^{-3} (θ_O for a Langmuir–Hinshelwood mechanism, n_O for an Eley–Rideal mechanism), r is the reaction rate in mol m^{-2} s^{-1}, k the rate constant, A the pre-exponential factor, T the grain temperature in K and $\Delta E^{\ddagger}$ the activation energy in K, while the subscripts 'rxn' and 'des' indicate reaction and desorption, respectively.

According to the results presented here, the Eley–Rideal mechanism ($^3O_g + CO_{ads}$) will never be an efficient route to CO_2 formation in the interstellar medium, because the activation barrier for reaction (2280 K) is larger than the energy of desorption (experimental $\Delta H^{\ddagger}_{\rm des} = 1560$ K, Ulbricht et al. 2006) and hence CO is always more likely to desorb than to react with ^3O_g as the grain temperature increases. In addition, the bimolecular pre-exponential factor for reaction ($\sim 10^7$ mol^{-1} m^3 s^{-1}, Atkins & De Paula 2006) multiplied by a typical oxygen pressure found in the interstellar medium ($n_O = 6 \times 10^{-18}$ mol m^{-3}, Stantcheva & Herbst 2004) is very much lower than the experimental pre-exponential factor for desorption (2×10^{14} s^{-1}; Ulbricht et al. 2006). Both factors adversely affect the reaction/desorption ratio shown in equation (4) and lead to the conclusion that the reaction between adsorbed CO and gas-phase oxygen atoms is not likely to occur.

The hot-atom or Langmuir–Hinshelwood mechanism is a more plausible route to CO_2 formation via equation (1). To evaluate the ratio of the rate of reaction and rate of desorption seen in equation (4), the pre-exponential factor is calculated from the harmonic frequencies for CO_{ads} and the transition state using Eyring (1938) transition state theory:

$$k_{\rm rxn} = \frac{k_{\rm b}T}{h}\frac{q^{\ddagger}}{q_{\rm COads}\Phi_{\rm COads,O}}\exp\left(\frac{-\Delta H^{\ddagger}_{\rm rxn}}{T}\right). \quad (5)$$

In this expression, the pre-exponential factor is $k_bT/h \times q^{\ddagger}/(q_{COads}\Phi_{COads,O})$, where $q^{\ddagger}$ and q_{COads} are the partition functions of the transition state and CO_{ads} and $\Phi_{COads,O}$ is the relative translational partition function per unit area, given by $(2\pi m_O k_b T/h^2)$ for an infinitely heavy surface. For a surface reaction, only the vibrations of the surface and adsorbate contribute to the ratio $q^{\ddagger}/q_{COads}$. The pre-exponential factor for the Langmuir–Hinshelwood or hot-atom reaction thus calculated ranges from 2.7×10^{15} mol^{-1} m^2 s^{-1} at 10 K to 6.4×10^{15} mol^{-1} m^2 s^{-1} at 100 K.

With the experimental parameters for desorption of CO from graphite ($\Delta H^{\ddagger}_{\rm des} = 1560$ K, $A_{\rm des} = 2 \times 10^{14}$ s^{-1}) and the calculated reaction parameters ($\Delta H^{\ddagger}_{\rm rxn} = 1580$ K, $A_{\rm rxn} = 4 \times 10^{15}$ mol^{-1} m^2 s^{-1}), CO_2 formation via the Langmuir–Hinshelwood or hot-atom mechanism is still heavily disfavoured ($<1{:}10^3$) over CO desorption, even if the surface is entirely covered with oxygen atoms ($\theta_O = 10^{-5}$ mol m^{-2}).

For the $^3O + CO_{ads}$ reaction to become an effective route, CO needs to be trapped in water ice, increasing its residence time on the grain (Collings et al. 2004). The first-order desorption parameters for H_2O adsorbed on graphite are $A_{\rm des} = 9 \times 10^{14}$ s^{-1} and $\Delta E^{\ddagger}_{\rm des} = 5530$ K (Ulbricht et al. 2006), while bulk water has a desorption energy of 4800 K (Brown & Bolina 2007). Using the experimental parameters from Ulbricht et al. for the desorption in equation (4), CO_{ads} is much more likely ($>10^6$:1) to react with O via either the Langmuir–Hinshelwood or hot-atom mechanism than to desorb at relevant temperatures (10–100 K), even for small oxygen surface concentrations of 10^{-9} mol m^{-2} ($\sim$0.01 per cent coverage). Because of the favourable value of the exponential term in equation (4), $(-\Delta E^{\ddagger}_{\rm rxn} + \Delta E^{\ddagger}_{\rm des})/T = 3970\,{\rm K}/T$, the preference of adsorbed CO to react with O_{ads} rather than desorb is especially pronounced at low temperatures, even though the absolute reaction rates are smaller.

These findings are in agreement with the observations of Roser et al. (2001) that CO_2 only formed from CO $+^3O$ when the sample was capped with water ice before heating it in temperature-programmed desorption. At a typical temperature of $T = 15$ K, with coverages of $\theta_{CO} = 10^{-7}$ mol m^{-2} (1 per cent) and $\theta_O = 10^{-8}$ mol m^{-2} (0.1 per cent), the rate of CO_2 formation via the hot-atom mechanism ($^3O^*_{ads} + CO_{ads}$) is still quite low, 10^{-46} mol m^2 s^{-1}. However, if CO_{ads} is effectively trapped in water ice, $^3O_{ads} + CO_{ads}$ could produce CO_2 more effectively during the warm-up period of a nearby forming star. For example, with the above coverages at 60 K the rate for CO_2 formation via the hot atom mechanism is 10^{-12} mol m^{-2} s^{-1} while the rate for codesorption of trapped CO is only 10^{-32} mol m^{-2} s^{-1}. The rate constant for CO_2 formation could be further increased by quantum mechanical tunnelling through the barrier. Although tunnelling is usually not considered important for heavy atoms, recently a high transmission coefficient has been demonstrated for carbon at 8 K (Zuev et al. 2003). Similarly, tunnelling may considerably increase the reaction rate for $^3O + CO$ at 10–100 K.

Reaction (2) is a viable route to CO_2 formation in the gas phase as well as on the carbonaceous surface, so long as the considerable excess energy of the first step ($O + HCO \rightarrow HCO_2$) is not completely transferred to the surface instantaneously. Since the HCO_2 intermediate is physisorbed, intramolecular energy transfer to the surface is unlikely to be fast enough to dissipate all of the excess energy before the intermediate will dissociate to yield $H + CO_2$.

As established experimentally, reaction (3) is a viable route to CO_2 formation in the gas phase down to 80 K (Frost et al. 1993). No measurements have yet been made at the very low temperatures (10–20 K) relevant to molecular clouds, but if the exit channel barrier is indeed higher in energy than the entrance barrier (Yu et al. 2001), the formation of CO_2 via OH + CO would be improbable in the

cold interstellar medium in the gas phase as well as on the surface. Instead, the reaction would halt at the intermediate HOCO, which in its turn can react with other radicals such as hydrogen. While the classical slowing of rates with temperature lowering could be counteracted by tunnelling of the departing hydrogen atom through the exit barrier (Chen & Marcus 2005), quantum dynamics calculations indicate that the rate is slowed upon lowering collision energies (Valero & Kroes 2006). When the OH + CO addition occurs on the carbonaceous surface, it is conceivable that the adsorbed HOCO intermediate will be stabilized by transfer of part of the excess energy to the surface. In that case, the exit barrier for removal of the hydrogen atom will be effectively heightened, inhibiting CO_2 formation. The HOCO radical thus formed will, however, react in a barrierless process with the next incoming hydrogen atom, the formation products depending on the orientation of the two reacting species. Statistically, about one third of these incidents will yield $H_2 + CO_2$.

Recently, more insight has been gained into the formation routes of CO_2 during different evolutionary stages in dark quiescent clouds through observations with the *Spitzer Space Telescope* (Pontoppidan 2006; Whittet et al. 2007). There appear to be two distinct phases in the formation of CO_2. In the early stages, CO_2 forms concomitantly with H_2O on the surface of dust grains, giving rise to a component of the CO_2 bending mode characteristic of a polar environment, while the second stage encompasses CO_2 formation occurring during the freeze-out of CO, yielding an apolar component.

From our calculations, we envisage two possible routes for the early-stage formation of CO_2. First, CO_2 and CO can be formed by energetic collisions (photons, cosmic rays) with water on a carbonaceous surface (Mennella, Palumbo & Barata 2004; Mennella et al. 2006). Alternatively, as water is being formed on the surface, via sequential hydrogenation ($O_{ads} + H \rightarrow OH_{ads} + H \rightarrow H_2O_{ads}$), CO could react with the OH intermediate via reaction (3). If the nascent OH_{ads} is formed in the vicinity of CO that is already frozen out, it would be quite likely to react.

In the second stage of the formation (apolar CO_2 component), CO_2 could form via reaction (1) on the CO ice, although the reaction probability would have to be increased either by trapping of the oxygen atoms in the ice, tunnelling through the barrier, or both. Alternatively, at this later stage, the OH + CO reaction could also occur, through the same chain of events as suggested for the early stages: $O + H \rightarrow OH + CO \rightarrow HOCO + H \rightarrow CO_2 + H_2$. In this scenario, the different concentration of CO in the two stages determines the likeliness of OH to react with CO or with another H: at the early stages, there is relatively little CO frozen out, leading to predominantly H_2O with CO_2 mixed in. In the later stages, when large amounts of CO have frozen out, every O that does not react directly with CO will be hydrogenated to OH and react with CO through equation (3) to eventually yield CO_2, via the net reaction $O + 2H + CO \rightarrow CO_2 + H_2$.

In summary our calculations suggest the following for existing chemical gas–grain networks.

(1) The $^3O + CO_{ads}$ addition reaction, which has a barrier of 1580 K for the hot-atom mechanism on a coronene surface, is likely to take place only in water ices where CO is trapped during the warm-up of a nearby forming star.

(2) On a carbonaceous surface the $OH_{ads} + CO_{ads}$ reaction yields an HOCO-intermediate. This intermediate is likely to be stabilized by intramolecular energy transfer to the surface, but it can subsequently react in a barrierless manner with an additional H to yield HCO_2H, $H_2 + CO_2$ or $H_2O + CO$ (all adsorbed).

ACKNOWLEDGMENTS

The EPSRC is acknowledged for a post-doctoral fellowship for TPMG and for computer resources on HPCx used through the Materials Chemistry and UKCP consortia. We also thank the RI and the STFC for use of their computer resources. Serena Viti is acknowledged for helpful discussions. We would also like to thank the referee for helpful comments. This work forms part of the research currently being undertaken in the UCL Centre for Cosmic Chemistry and Physics.

REFERENCES

Adamo C., Barone V., 1998, J. Chem. Phys., 108, 664
Allamandola L. J., Bernstein M. P., Sanford S. A., 1997, in Cosmovici C. B., Bowyer S., Wertheimer D., eds, Astronomical and Biochemical Origins and the Search for Life in the Universe. Editrici Compositori, Bologna, Italy, p. 23
Andersson S., Grüning M., 2004, J. Phys. Chem. A, 108, 7621
Andersson S., Al-Halabi A., Kroes G.-J., van Dishoeck E. F., 2006, J. Chem. Phys., 124, 064715
Atkins P., De Paula J., 2006, Physical Chemistry, 8th edn. Oxford Univ. Press, Oxford
Baulch D. L. et al., 2005, J. Phys. Chem. Ref. Data, 34, 757
Boonman A. M. S., van Dishoeck E. F., Lahuis F., Doty S. D., 2003, A&A, 399, 1063
Bonfanti M., Martinazzo R., Tantardini G. F., Ponti A., 2007, J. Phys. Chem. C, 111, 5825
Brown W. A., Bolina A. S., 2007, MNRAS, 374, 1006
Campbell I. M., Handy B. J., 1978, J. Chem. Soc. Faraday Trans. 1, 74, 316
Chen W.-C., Marcus R. A., 2005, J. Chem. Phys., 123, 094307
Collings M. P., Anderson M. A., Chen R., Dever J. W., Viti S., Williams D. A., McCoustra M. R. S., 2004, MNRAS, 354, 1133
d'Hendecourt L. B., Allamandola L. J., Grim R. J. A., Greenberg J. M., 1986, A&A, 158, 119
d'Hendecourt L. B., Jourdain de Muizon M., 1989, A&A, 223, L5
Eyring H., 1938, Trans. Faraday Soc. 34, 41
Fabian W. M. F., Janoschek R., 2005, THEOCHEM, 713, 227
Fournier J., Deson J., Verneil C., Pimentel G. C., 1979, J. Chem. Phys., 70, 5726
Frisch M. J. et al., 2004, GAUSSIAN 03, Revisions C.02 & D.01
Frost M. J., Sharkey P., Smith I. W. M., 1993, J. Phys. Chem., 97, 12254
Fujii N., Kakuda T., Takeishi N., Miyama H., 1987, J. Phys. Chem., 91, 2144
Fulle D., Hamann H. F., Hippler H., Troe J., 1996, J. Chem. Phys., 95, 983
Gerakines P. A., Schutte W. A., Ehrenfreund P., 1996, A&A, 312, 289
Gerakines P. A. et al., 1999, ApJ, 522, 357
Golden D. M. et al., 1998, J. Phys. Chem. A, 102, 8598
Grim R. J. A., d'Hendecourt L. B., 1986, A&A, 167, 161
Grim R. J. A., Greenberg J. M., de Groor M. S., Baas F., Schuttle W. A., Schmitt B., 1989, A&AS, 78, 161
Hamprecht F. A., Cohen A. J., Tozer D. J., Handy N. C., 1998, J. Chem. Phys., 109, 6264
Lynch B. J., Fast P. L., Harris M., Truhlar D. G., 2000, J. Phys. Chem. A, 104, 4811
Madzunkov S., Shortt B. J., MacAskill J. A., Darrach M. R., Chutjian A., 2006, Phys. Rev. A, 73, 020901
Mennella V., Palumbo M. E., Barata G. A., 2004, ApJ, 615, 1073
Mennella V., Barata G. A., Palumbo M. E., Bergin E. A., 2006, ApJ, 643, 923
Moore M. H., Khanna R., Donn B., 1991, J. Geophys. Res., 96, 17541
Piper J., Morrison J. A., Peters C., 1984, Mol. Phys., 53, 1463
Pontoppidan K. M., 2006, A&A, 453, L47
Roser J. E., Vidali G., Manicò G., Pirronello V., 2001, ApJ, 555, L61
Ruffle D. P., Herbst E., 2001, MNRAS, 324, 1054
Scott A., Duley W. W., 1996, ApJ, 472, L123
Song X., Li J., Hou H., Wang B., 2006, J. Chem. Phys., 125, 094301
Stantcheva T., Herbst E., 2004, A&A, 423, 241

Talbi D., Chandler G. S., Rohl A. L., 2006, Chem. Phys., 320, 214
Tsang W., Hampson R. F., 1986, J. Phys. Chem. Ref. Data, 15, 1087
Ulbricht H., Zacharia R., Cindir N., Hertel T., 2006, Carbon, 44, 2931
Valero R., Kroes G.-J., 2006, Chem. Phys. Lett., 417, 43
van Dishoeck E. F. et al., 1996, A&A, 315, L349
Whittet D. C. B. et al., 1998, ApJ, 498, L159
Whittet D. C. B., Shenoy S. S., Bergin E. A., Chiar J. E., Gerakires P. A., Gibb E. L., Melnick G. J., Neufield D. A., 2007, ApJ, 655, 332
Yu H.-G., Muckerman J. T., Sears T. J., 2001, Chem. Phys. Lett., 349, 547
Zhao Y., Truhlar D. G., 2004, J. Phys. Chem. A, 108, 6908
Zhao Y., Truhlar D. G., 2005, J. Phys. Chem. A, 109, 5656
Zuev P. S., Sheridan R. S., Albu T. V., Truhlar D. G., Hrovat D. A., Borden W. T., 2003, Sci, 299, 867

This paper has been typeset from a TEX/LATEX file prepared by the author.